International Scholarly Research Network
ISRN Analytical Chemistry
Volume 2012, Article ID 397026, 11 pages
doi:10.5402/2012/397026

Research Article

Vibrational Spectroscopic Study of (E)-4-(Benzylideneamino)-N-Carbamimidoyl Benzenesulfonamide

Asha Chandran,[1] Sheena Mary,[2] Hema Tresa Varghese,[2] C. Yohannan Panicker,[3,4] T. K. Manojkumar,[5] Christian Van Alsenoy,[6] and G. Rajendran[7]

[1] *Department of Chemistry, TKM College of Arts and Science, Kollam 695 005, Kerala, India*
[2] *Department of Physics, Fatima Mata National College, Kollam 695 001, India*
[3] *Department of Physics, TKM College of Arts and Science, Kollam 695 005, India*
[4] *Department of Physics, Research Centre, Mar Ivanios College, Nalanchira, Thiruvananthapuram 695015, India*
[5] *Indian Institute of Information Technology and Management-Kerala, Technopark, Thiruvananthapuram 695581, India*
[6] *Department of Chemistry, University of Antwerp, 2610 Antwerp, Belgium*
[7] *Department of Chemistry, University College Thiruvananthapuram, Thiruvananthapuram 695034, India*

Correspondence should be addressed to C. Yohannan Panicker, cyphyp@rediffmail.com

Received 8 September 2011; Accepted 13 October 2011

Academic Editors: S. E. Jorge-Villar and A. Taga

Copyright © 2012 Asha Chandran et al. This is an open access article distributed under the Creative Commons Attribution License, which permits unrestricted use, distribution, and reproduction in any medium, provided the original work is properly cited.

The Fourier transform infrared and Fourier transform Raman spectra of (E)-4-(benzylideneamino)-N-carbamimidoyl benzenesulfonamide were recorded and analyzed. Geometry and harmonic vibrational wavenumbers were calculated theoretically using Gaussian 03 set of quantum chemistry codes. Calculations were performed at the Hartree-Fock (HF) and density functional theory (DFT; B3PW91, B3LYP) levels of theory. The calculated wavenumbers (B3LYP) agree well with the observed wavenumbers. Potential energy distribution is done using GAR2PED program. The red shift of the N-H stretching band in the infrared spectrum from the computed wavenumber indicates the weakening of the N-H bond. The geometrical parameters of the title compound are in agreement with that of reported similar derivatives. The calculated first hyperpolarizability is comparable with the reported value of similar derivative and may be an attractive object for further studies of nonlinear optics. Potential energy surface scan studies have been carried out to understand the stability of planar and nonplanar structures of the molecule.

1. Introduction

Benzenesulfonamide derivatives find wide applications for the synthesis of pharmaceutical products which have bactericidal properties and of various bioactive agents, artificial fibers, dyes, and plasticizers, and the synthesis of high molecular weight substances. Sulfonamides are chemotherapeutics most commonly used in veterinary practices because of their inexpensiveness and wide spectrum antimicrobial activity [1]. Sulfonamides represent one of the classical chemotypes associated with potent CA inhibition [2–5]. The chemistry of sulfonamides has been known as synthons in the preparation of various valuable biologically active compounds [6, 7] used as an antibacterial [8], protease inhibitor [9], diuretic [10], antitumor [11], and hypoglycaemic [12]. Singh et al. [13] reported the synthesis and antimicrobial activity of Schiff's and N-Mannich bases of Isatin and its derivatives with 4-amino-N-carbamimidoyl benzene sulfonamide. There has been growing interest in using organic materials for nonlinear optical (NLO) devices, functioning as second harmonic generators, frequency converters, electro-optical modulators, and so forth because of the large second order electric susceptibilities of organic materials. The organic compound showing high hyperpolarizability are those containing an electron-donating group and an electron-withdrawing group interacting through a system of conjugated double bonds. In the case of sulfonamides, the electron-withdrawing group is the sulfonyl group [14, 15]. To our knowledge, no theoretical

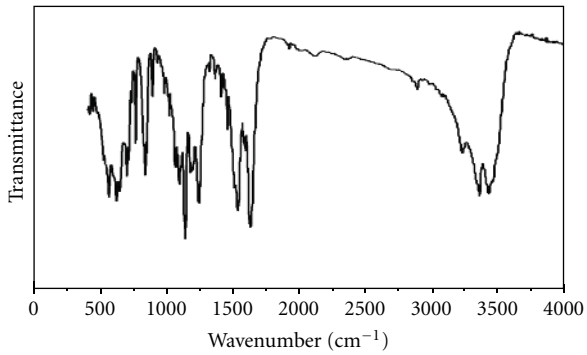

Figure 1: FT-IR spectrum of (E)-4-(benzylideneamino)-N-carbamimidoyl benzenesulfonamide.

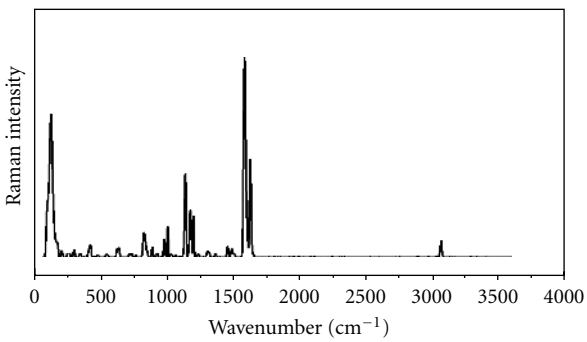

Figure 2: FT-Raman spectrum of (E)-4-(benzylideneamino)-N-carbamimidoyl benzenesulfonamide.

HF or density functional theory (DFT) calculations or detailed vibrational infrared or Raman analyses have been performed on the title compound.

2. Experimental

All the chemicals were procured from Sigma-Aldrich, USA. 0.5 mg of sulphaguanidine and 0.3 mL of benzaldehyde in 20 mL ethyl alcohol are refluxed for 3 hrs. The white precipitate was filtered off, washed with ethanol, and dried. Elemental analysis: found/calculated (%): C 55.50/55.63; H 4.59/4.63; N 18.40/18.50; S 10.58/10.59. The FT-IR spectrum (Figure 1) was recorded on a DR/Jasco FT-IR 6300 spectrometer in KBr pellets, number of scans 16, resolution 2 cm^{-1}. The FT-Raman spectrum (Figure 2) was obtained on a BRUKER RFS 100/S, Germany. For excitation of the spectrum the emission of an Nd:YAG laser was used, excitation wavelength 1064 nm, maximal power 150 mW, measurement of solid sample. One thousand scans were accumulated with a total registration time of about 30 min. The spectral resolution after apodization was 2 cm^{-1}.

3. Computational Details

Calculations of the title compound were carried out with Gaussin 03 program [16] using the HF/6-31G*, B3PW91/6-31G* and B3LYP/6-31G*, basis sets to predict the molecular structure and vibrational wavenumbers. The wavenumber values computed contain known systematic errors [17] and we, therefore, have used the scaling factor values of 0.8929 and 0.9613 for HF and DFT basis sets. Parameters corresponding to optimized geometry (B3LYP) of the title compound (Figure 3) are given in Table 1. The absence of imaginary values of wavenumbers on the calculated vibrational spectrum confirms that the structure deduced corresponds to minimum energy. Potential energy distribution is done using GAR2PED program [18]. The assignment of the calculated wavenumbers is aided by the animation option of MOLEKEL program, which gives a visual presentation of the vibrational modes [19, 20]. Potential energy surface scan studies have been carried out to understand the stability of planar and non planar structures of the molecule. The profiles of potential energy surface for torsion angles C_{15}–N_{14}–C_{12}–C_3, N_{28}–S_{25}–C_{22}–C_{20}, N_{31}–C_{30}–N_{28}–S_{25} and N_{32}–C_{30}–N_{28}–S_{25} are given in Figures 4–7. The energy is minimum for −177.0 (−1309.42093 Hartree), 86.0 (−1309.41690 Hartree), 12.6 (−1309.42098 Hartree), and −169.9 (−1309.42070 Hartree) for the above torsion angles.

4. Results and Discussion

4.1. IR and Raman Spectra. The observed IR, Raman bands, and calculated (scaled) wavenumbers, and assignments are given in Table 2.

The asymmetric and symmetric stretching modes of SO_2 group appear in the region 1360–1310 and 1165–1135 cm^{-1} [21]. The observed bands at 1358, 1130 cm^{-1} in the IR spectrum, 1360, 1133 cm^{-1} in the Raman spectrum, and 1371, 1148 cm^{-1} theoretically are assigned as SO_2 stretching modes. These modes are not pure, but contain significant contributions from other modes also. Although the region of SO_2 scissors (560 ± 40 cm^{-1}) and that of SO_2 wagging (500 ± 55 cm^{-1}) partly overlap, the two vibrations appear separately [21]. These deformation bands of SO_2 are assigned at 515, 469 cm^{-1} in the IR spectrum and at 510, 457 cm^{-1} theoretically. Chohan et al. [22] reported the SO_2 stretching vibrations at 1345, 1110 cm^{-1} and SN and CS stretching modes at 833 cm^{-1} for sulfonamide derivatives. Hangen et al. [23] reported SO_2 modes at 1314, 1308, 1274, 1157, 1147, and 1133 cm^{-1} and SN stretching modes at 917, 920, 932, and 948 cm^{-1} for sulfonamide derivatives. The twisting mode of SO_2 is expected at around 350 cm^{-1} [21]. The calculated bands (B3LYP) at 365, 298 cm^{-1} are assigned as the twisting and rocking modes of SO_2. The NS stretching vibration is expected [21] in the region 905 ± 30 cm^{-1} and the band observed at 841 cm^{-1} in the IR spectrum and at 831 cm^{-1} theoretically are assigned as υSN. The C–S stretching vibration is assigned at 692 cm^{-1} (IR) and at 679 cm^{-1} (DFT) cm^{-1} [21].

The C=N stretching bands [24] are observed in the region 1550–1700 cm^{-1} and for the title compound, the B3LYP calculation give these bands at 1687(C_{12}–N_{14}), 1641 cm^{-1} (C_{30}–N_{31}). The CN stretching vibrations [21] are moderately to strongly active in the region 1275 ± 55 cm^{-1}. Primary aromatic amines with nitrogen directly on the ring absorb at 1330–1200 cm^{-1} because of the stretching of the phenyl

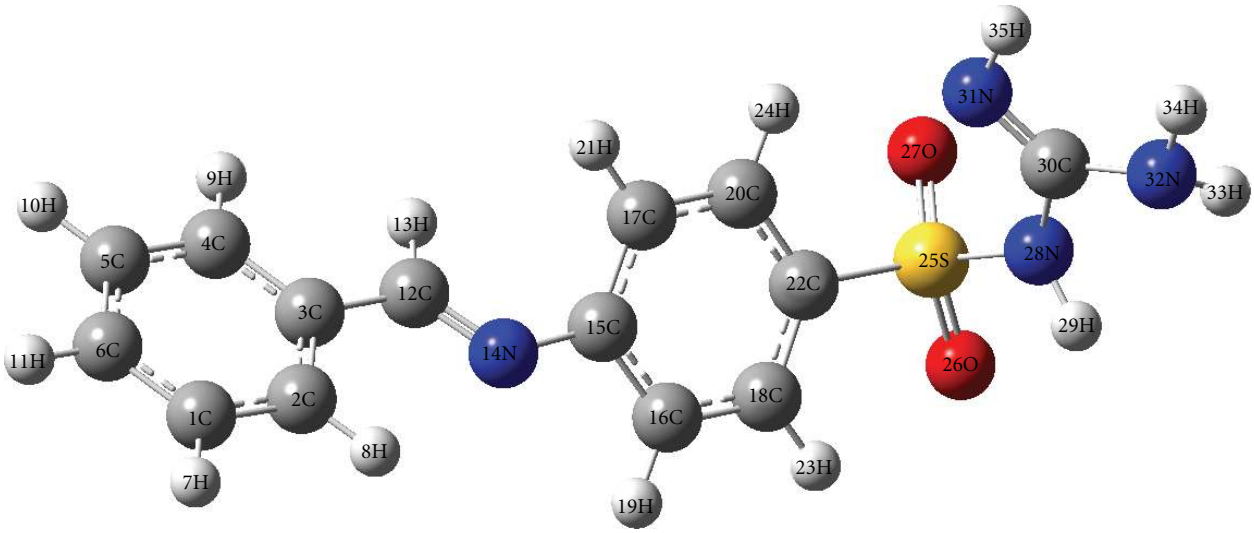

Figure 3: Optimized geometry (B3LYP) of (E)-4-(benzylideneamino)-N-carbamimidoyl benzene sulfonamide.

carbon nitrogen bond [25]. For the title compound C_{15}–N_{14} stretching mode is observed at 1281 cm^{-1} theoretically. Panicker et al. [26] reported the CN stretching modes at 1219, 1237 cm^{-1} (IR), 1222 cm^{-1} (Raman) and at 1292, 1234, 1200 cm^{-1} theoretically. The CN stretching modes C_{30}–N_{28} and C_{30}–N_{32} are assigned at 1100 and 942 cm^{-1} theoretically which is expected in the range 950–1115 cm^{-1} [21].

The NH_2 stretching modes are expected in the region 3260–3390 cm^{-1} [21] and in the present case the bands observed at 3421 cm^{-1} in the IR spectrum and bands at 3501, 3399 cm^{-1} (DFT) are assigned as NH_2 stretching modes. The bands corresponding to δNH_2 vibrations are expected in the region 1610 ± 30 cm^{-1} [21]. In the present case, the band at 1620 cm^{-1} (IR), 1625 cm^{-1} (Raman) and 1602 cm^{-1} (DFT) is assigned as δNH_2. The rocking/twisting mode of NH_2 is expected in the region 1195 ± 90 cm^{-1} and this mode is assigned at 1182 cm^{-1} in IR, 1188 cm^{-1} in Raman spectrum at 1181 (DFT) cm^{-1}. The wagging mode of NH_2 is assigned at 778 cm^{-1} theoretically which is expected in the region 840 ± 55 cm^{-1} [21]. The torsional NH_2 mode is expected below 400 cm^{-1} [21] and these modes are identified and assigned (Table 2). For sulfonamide derivatives the NH_2 modes are reported at 3390, 3395, at 3399 cm^{-1} [22].

The NH stretching vibrations generally give rise to bands at 3500–3300 cm^{-1} [27, 28]. In the present study, the N_{28}–H_{29} stretching bands have split into a doublet, 3351, 3222 cm^{-1} in the IR spectrum owing to the Davydov coupling between neighboring units. The splitting of about 129 cm^{-1} in the IR spectrum is due to the strong intermolecular hydrogen bonding. Furthermore the NH stretching wave number is red shifted by 129 cm^{-1} in the IR spectrum with a strong intensity from the computed wavenumber which indicate the weakening of the NH bond [29]. The DFT calculations give the N_{31}–H_{35} stretching mode at 3453 cm^{-1}. In N-mono substituted amides, the in plane bend ing frequency and the resonance stiffened CN bands stretching frequency fall close together and therefore interact. The NH deformation band of guanidine structural motif is expected in the region 1395 ± 25 cm^{-1} [21, 25]. The DFT calculations give these modes at 1442 and 1485 cm^{-1}. The bands observed at 1500, 1450 cm^{-1} in the IR spectrum and at 1486, 1446 cm^{-1} in the Raman spectrum are assigned as the deformation bands of NH group. The out-of-plane NH deformation is expected in the region 650 ± 50 cm^{-1} [21] and bands at 727 (IR), 729 (Raman) and 706, 608 cm^{-1} (DFT) are assigned as these modes.

Since the identification of all the normal modes of vibration of large molecules is not trivial, we tried to simplify the problem by considering each molecule as a substituted benzene. Such an idea has already been successfully utilized by several workers for the vibrational assignments of molecules containing homo- and heteroaromatic rings [30–32]. In the following discussion, mono- and parasubstituted phenyl rings are designated as PhI and PhII, respectively. The modes in the phenyl rings will differ in wavenumber and the magnitude of splitting will depend on the strength of the interactions between different parts (internal coordinates) of the two rings. For some modes, this splitting is so small that they may be considered as quasidegenerate, and for some other modes a significant amount of splitting is observed. Such observations have already been reported [33, 34].

The phenyl CH stretching modes occur above 3000 cm^{-1} and are typically exhibited as multiplicity of weak to moderate bands compared with the aliphatic CH stretching [35]. In the present case, the DFT calculations give υCH modes of the phenyl rings in the range 3132–3057 cm^{-1}. The bands observed at 3026, 3073 cm^{-1} in the IR spectrum and at 3066 cm^{-1} in the Raman spectrum were assigned as CH stretching modes of the phenyl rings.

The benzene ring possesses six ring stretching vibrations, of which the four with the highest wavenumbers (occurring near 1600, 1580, 1490, and 1440 cm^{-1}) are good group vibrations. With heavy substituents, the bands tend to shift to somewhat lower wavenumbers. In the absence of ring conjugation, the band at 1580 cm^{-1} is usually weaker than that at 1600 cm^{-1}. In the case of C=O substitution, the band

Table 1: Geometrical (B3LYP) parameters of (E)-4-(benzylideneamino)-N-carbamimidoyl benzenesulfonamide, atom labeling according to Figure 3.

Bond lengths (Å)		Bond angles (°)		Dihedral angles (°)	
C_1–C_2	1.3901	A(2,1,6)	120.2	D(6,1,2,3)	−0.0
C_1–C_6	1.4001	A(2,1,7)	119.8	D(6,1,2,8)	−180.0
C_1–H_7	1.0866	A(6,1,7)	119.9	D(7,1,2,3)	180.0
C_2–C_3	1.4062	A(1,2,3)	120.1	D(7,1,2,8)	0.0
C_2–H_8	1.0852	A(1,2,8)	121.3	D(2,1,6,5)	0.1
C_3–C_4	1.4035	A(3,2,8)	118.6	D(2,1,6,11)	−180.0
C_3–C_{12}	1.4666	A(2,3,4)	119.2	D(7,1,6,5)	−180.0
C_4–C_5	1.3941	A(2,3,12)	121.5	D(7,1,6,11)	0.0
C_4–H_9	1.0878	A(4,3,12)	119.3	D(1,2,3,4)	−0.0
C_5–C_6	1.3958	A(3,4,5)	120.5	D(1,2,3,12)	180.0
C_5–H_{10}	1.0864	A(3,4,9)	119.4	D(8,2,3,4)	179.9
C_6–H_{11}	1.0867	A(5,4,9)	120.0	D(8,2,3,12)	−0.2
C_{12}–H_{13}	1.1006	A(4,5,6)	119.8	D(2,3,4,5)	0.1
C_{12}–N_{14}	1.2816	A(4,5,10)	120.0	D(2,3,4,9)	−179.9
C_{15}–N_{14}	1.4020	A(6,5,10)	120.2	D(12,3,4,5)	−179.8
C_{15}–C_{16}	1.4061	A(1,6,5)	120.0	D(12,3,4,9)	0.2
C_{15}–C_{17}	1.4078	A(1,6,11)	120.0	D(2,3,12,13)	−179.7
C_{16}–C_{18}	1.3893	A(5,6,11)	120.0	D(2,3,12,14)	1.1
C_{16}–H_{19}	1.0854	A(3,12,13)	115.6	D(4,3,12,13)	0.2
C_{17}–C_{20}	1.3912	A(3,12,14)	122.8	D(4,3,12,14)	−179.0
C_{17}–H_{21}	1.0859	A(13,12,14)	121.6	D(3,4,5,6)	−0.1
C_{18}–C_{22}	1.3991	A(12,14,15)	120.1	D(3,4,5,10)	180.0
C_{18}–H_{23}	1.0845	A(14,15,16)	117.8	D(9,4,5,6)	180.0
C_{20}–C_{22}	1.3968	A(14,15,17)	123.0	D(9,4,5,10)	−0.0
C_{20}–H_{24}	1.0827	A(16,15,17)	119.2	D(4,5,6,1)	−0.0
C_{22}–S_{25}	1.7883	A(15,16,18)	120.5	D(4,5,6,11)	−180.0
S_{25}–O_{26}	1.4658	A(15,16,19)	118.6	D(10,5,6,1)	180.0
S_{25}–O_{27}	1.4570	A(18,16,19)	120.8	D(10,5,6,11)	−0.0
S_{25}–N_{28}	1.7054	A(15,17,20)	120.7	D(3,12,14,15)	−177.0
N_{28}–H_{29}	1.0140	A(15,17,21)	119.6	D(13,12,14,15)	3.8
C_{30}–N_{28}	1.4033	A(20,17,21)	119.7	D(12,14,15,16)	−140.4
C_{30}–N_{31}	1.2764	A(16,18,22)	119.3	D(12,14,15,17)	42.1
C_{30}–N_{32}	1.3990	A(16,18,23)	120.9	D(14,15,16,18)	−179.6
N_{31}–H_{35}	1.0208	A(22,18,23)	119.8	D(14,15,16,19)	1.7
N_{32}–H_{33}	1.0149	A(17,20,22)	119.1	D(17,15,16,18)	−2.1
N_{32}–H_{34}	1.0130	A(17,20,24)	121.2	D(17,15,16,19)	179.2
—	—	A(22,20,24)	119.7	D(14,15,17,20)	178.6
—	—	A(18,22,20)	121.2	D(14,15,17,21)	0.6
—	—	A(18,22,25)	118.7	D(16,15,17,20)	1.2
—	—	A(20,22,25)	120.1	D(16,15,17,21)	−176.8
—	—	A(22,25,26)	107.7	D(15,16,18,22)	1.6
—	—	A(22,25,27)	108.9	D(15,16,18,23)	−177.7
—	—	A(22,25,28)	107.7	D(19,16,18,22)	−179.6
—	—	A(26,25,27)	122.2	D(19,16,18,23)	1.0
—	—	A(26,25,28)	101.5	D(15,17,20,22)	−0.0
—	—	A(27,25,28)	108.0	D(15,17,20,24)	−178.6
—	—	A(25,28,29)	112.2	D(21,17,20,22)	178.0
—	—	A(25,28,30)	126.8	D(21,17,20,24)	−0.5
—	—	A(25,28,30)	117.8	D(16,18,22,20)	−0.4
—	—	A(28,30,31)	121.2	D(16,18,22,25)	−179.4

Table 1: Continued.

Bond lengths (Å)		Bond angles (°)		Dihedral angles (°)	
—	—	A(28,30,32)	110.2	D(23,18,22,20)	178.9
—	—	A(31,30,32)	128.6	D(23,18,22,25)	0.0
—	—	A(30,31,35)	111.1	D(17,20,22,18)	−0.4
—	—	A(30,32,33)	114.6	D(17,20,22,25)	178.5
—	—	A(30,32,34)	113.9	D(24,20,22,18)	178.2
—	—	A(33,32,34)	111.9	D(24,20,22,25)	−2.9
—	—	—	—	D(18,22,25,26)	13.7
—	—	—	—	D(18,22,25,27)	148.1
—	—	—	—	D(18,22,25,28)	−95.1
—	—	—	—	D(20,22,25,26)	−165.2
—	—	—	—	D(20,22,25,27)	−30.8
—	—	—	—	D(20,22,25,28)	86.0
—	—	—	—	D(22,25,28,29)	91.5
—	—	—	—	D(22,25,28,30)	−67.8
—	—	—	—	D(26,25,28,29)	−21.4
—	—	—	—	D(26,25,28,30)	179.3
—	—	—	—	D(27,25,28,29)	−151.1
—	—	—	—	D(27,25,28,30)	49.6
—	—	—	—	D(25,28,30,31)	12.6
—	—	—	—	D(25,28,30,32)	−169.9
—	—	—	—	D(29,28,30,31)	−145.7
—	—	—	—	D(29,28,30,32)	31.8
—	—	—	—	D(28,30,31,35)	−173.1
—	—	—	—	D(32,30,31,35)	9.8
—	—	—	—	D(28,30,32,33)	43.7
—	—	—	—	D(28,30,32,34)	174.5
—	—	—	—	D(31,30,32,33)	−139.0
—	—	—	—	D(31,30,32,34)	−8.2

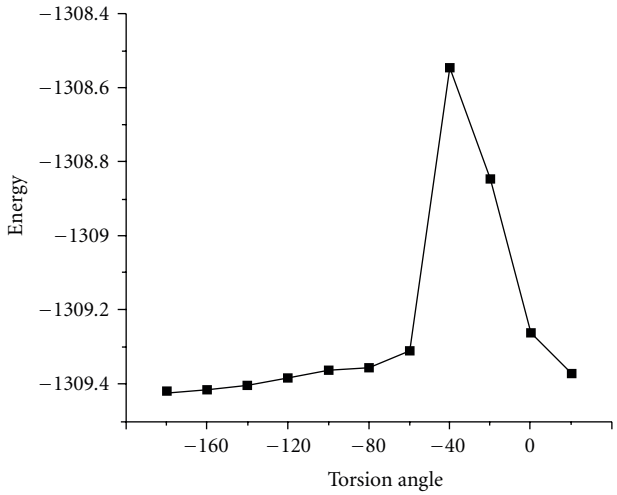

Figure 4: Profile of potential energy scan for the torsion angle C_{15}–N_{14}–C_{12}–C_3.

near 1490 cm^{-1} can be very weak. The fifth ring stretching vibration is active near 1315 ± 65 cm^{-1}, a region that overlaps strongly with that of the CH in-plane deformation. The sixth ring stretching vibration, or the ring breathing mode, appears as a weak band near 1000 cm^{-1}, in mono-, 1, 3-di-, and 1, 3, 5-trisubstituted benzenes. In the otherwise substituted benzenes, however, this vibration is substituent sensitive and difficult to distinguish from the ring in-plane deformation [21, 36].

The υPh modes are expected in the region 1285–1610 cm^{-1} and 1280–1630 cm^{-1} for PhI and PhII rings, respectively [21]. The DFT calculations give the Ph stretching modes in the range 1290–1598 cm^{-1} and 1265–1578 cm^{-1} for PhI and PhII, respectively. For the title compound the phenyl ring stretching modes are observed at 1567, 1500 (IR), 1581, 1486 cm^{-1} (Raman) and 1587, 1528, 1403, 1130 cm^{-1} (IR), 1133 cm^{-1} (Raman), for PhI and PhII, respectively. Most of the modes are not pure but contain significant contributions from other modes also. The ring breathing mode of the parasubstituted benzenes with entirely different substituents [36] has been reported in the interval 780–880 cm^{-1}. For the title c ompound, the ring breathing mode PhII is observed at 757 cm^{-1} in the IR spectrum which is supported by the computational result at 747 cm^{-1}. The ring breathing mode of PhI is observed at 1001 cm^{-1} in the Raman spectrum and the theoretical calculated value is

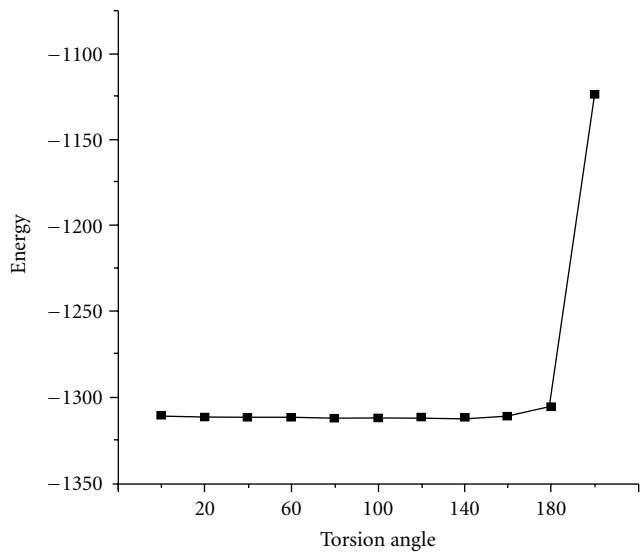

Figure 5: Profile of potential energy scan for the torsion angle N_{28}–S_{25}–C_{22}–C_{20}.

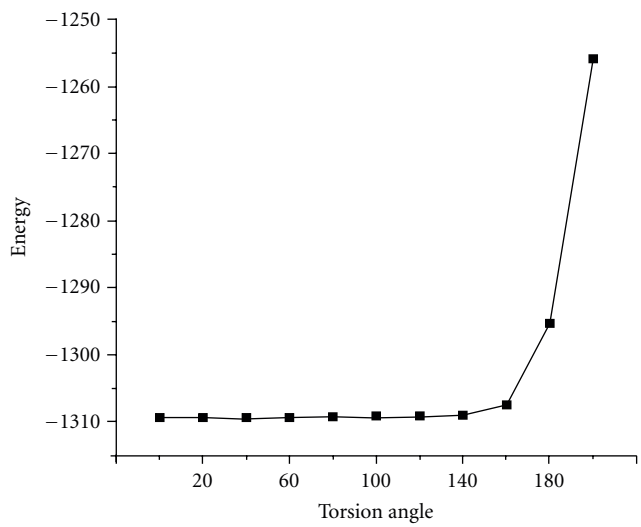

Figure 6: Profile of potential energy scan for the torsion angle N_{31}–C_{30}–N_{28}–S_{25}.

990 cm^{-1}, as expected [21]. The in-plane and out-of-plane CH deformation bands of the phenyl ring are expected above and below 1000 cm^{-1} [21]. The in-plane CH deformation bands are assigned at 1319, 1160, 1156, 1096, 1076, and 1013 cm^{-1} for PhI and at 1317, 1230, 1103, and 1044 cm^{-1} for PhII theoretically. The strong γCH occurring at 840 ± 50 cm^{-1} is typical for 1, 4-disubstituted benzenes and the band observed at 804 cm^{-1} in the IR spectrum is assigned to this mode [21]. The in-plane and out-of-plane deformation modes of the phenyl ring are also identified and assigned (Table 2).

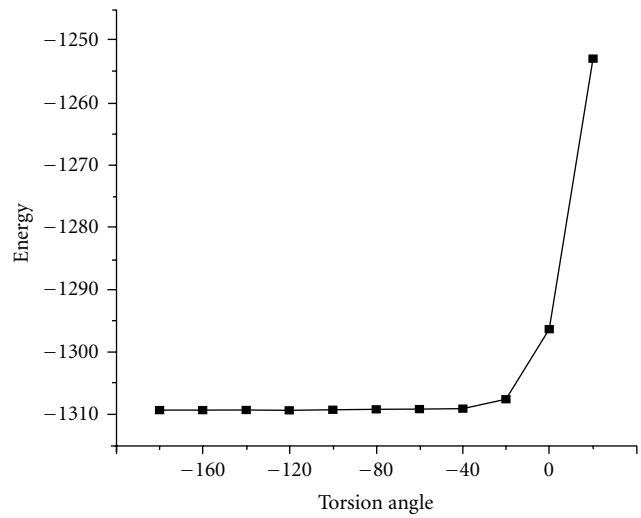

Figure 7: Profile of potential energy scan for the torsion angle N_{32}–C_{30}–N_{28}–S_{25}.

The IR bands in the region 2882–1915 cm^{-1} and their large broadening support the intramolecular hydrogen bonding [37].

4.2. Geometrical Parameters and First Hyperpolarizability. To the best of our knowledge, no X-ray crystallographic data of this molecule has yet been established. However, the theoretical results obtained are almost comparable with the reported structural parameters of the parent molecules.

Loughrey et al. [38] reported the bond lengths, S_{25}–O_{27} = 1.4337, S_{25}–O_{26} = 1.4256, S_{25}–N_{28} = 1.6051, S_{25}–C_{22} = 1.7737, C_{15}–N_{14} = 1.4212, C_{12}–N_{14} = 1.2712, whereas the corresponding values for the title compound are 1.4570, 1.4658, 1.7054, 1.7883, 1.4020, and 1.2816 Å. For the title compound, the DFT calculations give the bond angles, C_{22}–S_{25}–O_{27} = 108.9, C_{22}–S_{25}–O_{26} = 107.7, S_{25}–N_{28}–H_{29} = 112.2, O_{27}–S_{25}–O_{26} = 122.2, O_{27}–S_{25}–N_{28} = 108.0, O_{26}–S_{25}–N_{28} = 101.5, N_{28}–S_{25}–C_{22} = 107.7, C_{15}–N_{14}–C_{12} = 120.1, S_{25}–C_{22}–C_{18} = 118.7, S_{25}–C_{22}–C_{20} = 120.1, C_{22}–C_{18}–C_{16} = 119.3, C_{18}–C_{16}–C_{15} = 120.5, C_{16}–C_{15}–C_{17} = 119.2, N_{14}–C_{15}–C_{17} = 123.0, N_{14}–C_{15}–C_{16} = 117.8, C_{15}–C_{17}–C_{20} = 120.7, N_{14}–C_{12}–C_3 = 122.8°, whereas the corresponding reported values are 106.5, 107.4, 110.0, 119.5, 106.1, 107.7, 109.3, 118.8, 120.5, 119.1, 120.4, 119.9, 120.3, 119.3, 122.4, 118.2, 120.4, and 124.4° [38].

Loughrey et al. [38] reported the torsion angles, O_{27}–S_{25}–C_{22}–C_{18} = −142.0, O_{27}–S_{25}–C_{22}–C_{20} = 38.5, O_{26}–S_{25}–C_{22}–C_{18} = −12.8, O_{26}–S_{25}–C_{22}–C_{20} = 167.7, N_{28}–S_{25}–C_{22}–C_{18} = 103.8, N_{28}–S_{25}–C_{22}–C_{20} = −75.7, C_{12}–N_{14}–C_{15}–C_{16} = 143.9, C_{12}–N_{14}–C_{15}–C_{17} = −39.2, C_{15}–N_{14}–C_{12}–C_3 = 117.6, S_{25}–C_{22}–C_{18}–C_{16} = −179.9, C_{20}–C_{22}–C_{18}–C_{16} = −0.4, S_{25}–C_{22}–C_{20}–C_{17} = 179.2, C_{18}–C_{16}–C_{15}–N_{14} = 178.1, N_{14}–C_{15}–C_{17}–C_{20} = −178.6, N_{14}–C_{12}–C_3–C_2 = 8.1, N_{14}–C_{12}–C_3–C_4 = −172.6°. For the title compound, the corresponding torsion angles are 148.1, −30.8, 13.7, −165.2, −95.1, 86.0, −140.4,

Table 2: Calculated vibrational wavenumbers (scaled), measured infrared and Raman band positions, and assignments of (E)-4-(benzylideneamino)-N-carbamimidoyl benzenesulfonamide.

HF υ (cm^{-1})	B3PW91 υ (cm^{-1})	B3LYP υ (cm^{-1})	$\upsilon_{(IR)}$	$\upsilon_{(Raman)}$	Assignments
3563	3532	3501	—	—	$\upsilon_{as}NH_2$ (100)
3450	3476	3453	3459	—	$\upsilon N_{31}H_{35}$ (82)
3443	3426	3399	3421	—	$\upsilon_{s}NH_2$ (82)
3376	3381	3351	3351, 3222	—	$\upsilon N_{28}H_{29}$ (100)
3072	3136	3132	3073	—	υCH II (97)
3052	3115	3109	—	—	υCH II (99)
3042	3107	3100	—	—	υCH I (96)
3037	3098	3090	—	—	υCH II (99)
3027	3098	3087	—	—	υCH I (94)
3025	3089	3082	—	—	υCH II (97)
3014	3087	3076	—	—	υCH I (94)
3001	3076	3066	—	3066	υCH I (93)
2991	3067	3057	3026	—	υCH I (93)
2895	2923	2915	—	—	$\upsilon C_{12}H_{13}$ (99)
1683	1637	1687	—	—	$\upsilon C_{12}N_{14}$ (68)
1676	1655	1641	—	—	$\upsilon C_{30}N_{31}$ (60)
1640	1609	1602	1620	1625	δNH_2 (87)
1617	1603	1598	—	—	υPh I (53)
1600	1590	1578	1587	—	υPh II (58)
1590	1583	1571	1567	1581	υPh I (63)
1578	1564	1552	1528	—	υPh II (68)
1501	1487	1485	1500	1486	υPh I (42), δNH I (39)
1495	1473	1472	—	—	υPh II (60), δCH I (15), δCH II (20)
1472	1442	1442	1450	1446	δNH (65)
1456	1440	1430	—	—	υPh I (64), δCH I (34)
1407	1397	1394	1403	—	υPh II (57), δCH II (36)
1387	1370	1371	1358	1360	$\upsilon_{as}SO_2$ (60), δCH_{13} (28)
1334	1335	1319	—	—	δCH I (68)
1319	1332	1317	1313	1310	δCH II (84)
1310	1314	1299	—	—	δNH (56)
1242	1294	1290	—	—	υPh I (67), δCH I (17)
1233	1279	1281	—	—	υPh I (40), $\upsilon C_{15}N_{14}$ (58)
1215	1272	1265	—	—	υPh II (82)
1185	1236	1230	1236	1234	υPh II (14), δCH II (42)
1181	1187	1181	1182	1188	δCH I (36), δNH_2 (56)
1172	1159	1160	1170	1168	$\upsilon C_{15}N_{14}$ (18), δCH II (14), δCH I (60)
1148	1156	1156	—	—	δCH I (48), υPh I (40)
1107	1147	1148	1130	1133	$\upsilon_{s}SO_2$ (46), υPh II (46)
1086	1118	1103	—	—	δCH II (61), δNH_2 (28)
1078	1097	1100	—	—	$\upsilon C_{30}N_{28}$ (45), δNH_2 (36)
1074	1095	1096	1087	1088	δCH I (61), υPh I (38)
1066	1083	1076	—	—	δCH I (73)
1058	1071	1069	1057	1065	υPh II (46)
1045	1056	1044	—	—	δCH II (70)
1037	1017	1013	1010	1015	δCH I (63)
1035	990	990	—	1001	υPh I
1029	984	980	—	—	γCH II (69)
1020	980	978	971	974	γCH I (82)
1007	977	972	—	—	υPh II (81)

Table 2: Continued.

HF υ (cm^{-1})	B3PW91 υ (cm^{-1})	B3LYP υ (cm^{-1})	$\upsilon_{(IR)}$	$\upsilon_{(Raman)}$	Assignments
994	966	965	—	—	γCH I (80)
990	945	942	948	—	$\upsilon C_{30}N_{32}$ (68)
975	940	940	—	—	γCH I (74)
897	925	926	921	922	γCH II (79)
887	902	901	—	—	γCH I (99)
873	867	865	884	882	γCH II (89)
859	831	831	841	—	υSN (67)
847	830	823	829	820	γCH II (59), γCH_{13} (15)
809	819	819	—	—	γCH II (57), υPh I (12)
795	811	806	—	—	δNH (82)
789	800	802	796	—	γCH I (63)
782	776	778	—	—	δNH_2 (61)
748	745	747	757	751	υPh II (64)
715	707	706	727	729	γNH (69)
710	690	689	709	709	γCH I (25), δPh I (64)
694	678	679	692	—	υCS (58), δCN (23)
656	673	673	—	—	δSO_2 (40), δPh II (18)
636	619	621	633	629	δPh II (79)
626	612	610	612	610	δPh I (85)
602	605	608	—	—	γNH (65)
570	590	590	—	—	δPhI (29), δPhII (20), δCN (24)
554	575	579	—	—	τPhII (30), γCS (17), =CN (17)
521	542	541	556	543	τPhI (51), δCC_{12} (31)
510	530	529	—	—	δNH (46), δNH_2 (32)
478	509	510	515	—	δNH_2 (28), δSO_2 (47), δCN (14)
468	497	496	—	—	γNH_2 (41), τPhI (20)
442	455	457	469	460	δSO_2 (41), γNH (39)
427	424	419	435	—	τPhII (84)
419	405	407	408	415	τPhI (84)
413	399	401	—	—	δSO_2 (40) δPhII (31)
376	398	397	—	—	δCN (35), τPhII (33)
345	366	365	—	—	δSO_2 (47), δCS (24)
320	355	353	—	—	δSO_2 (39), τCC (25)
299	349	347	—	343	γNH (64), δSO_2 (15)
275	342	338	—	—	τNH (39), τPhI (36)
270	299	298	—	295	δSO_2 (40), τNH (23)
247	275	275	—	—	δSO_2 (50), γNH (28)
243	253	253	—	255	τSO_2 (36), δCN (31)
204	216	217	—	209	τSO_2 (48), τPhII (29)
162	177	179	—	—	τSO_2 (28), τNH (21), τCS (17)
156	160	160	—	—	δNH (47), τCN (26)
133	138	138	—	—	δNH (44), δSO_2 (25)
120	127	128	—	120	τCN (45), δSO_2 (38)
108	107	107	—	—	τNH (34), τCN (27)
80	82	81	—	—	τCN (38), τSO_2
59	55	55	—	—	τCN (38), δSO_2 (29)
49	48	48	—	—	τSO_2 (25), τCN (34)
41	43	42	—	—	τCN (53), τSO_2 (12)
25	24	24	—	—	τPh II (63), τCN(56), τSO_2 (21)
22	22	23	—	—	τSO_2 (39), τCN (24), τNH (10)

υ: stretching, δ: in-plane bending, γ: out-of-plane bending, τ: torsion, PhI: monosubstituted phenyl ring, PhII: parasubstituted phenyl ring. Subscripts: as: asymmetric; s: symmetric.

42.1, −177.0, −179.4, −0.4, 178.5, −179.6, 178.6, 1.1, and −179.0°.

Petrov et al. [39] reported the molecular structure and conformations of benzenesulfonamide by gas electron diffraction and quantum chemical calculations and according to their results, the bond lengths, CS, SN, SO vary in the range 1.7756–1.7930, 1.6630–1.6925, 1.4284–1.4450 Å the bond angles, CSN, CSO, NSO, HNS, HNH vary in the range, 103.9–107.1, 107.6–107.8, 105.5–107.7, 111.0–113.7, 112.6–113.6 Å. These values are in agreement with the corresponding values for the title compound.

Lasibal et al. [40] reported the bond lengths SO = 1.4269–1.4291, SN = 1.6202, SC = 1.7582, N_{32}–C_{30} = 1.4103, N_{31}–C_{30} = 1.2723, N_{28}–C_{30} = 1.3483 Å, whereas the corresponding values in the present case are 1.4658–1.4570, 1.7054, 1.7833, 1.3930, 1.2764, and 1.4033 Å. The values of bond angles O_{27}–S_{25}–O_{26} = 118.6, O_{26}–S_{25}–N_{28} = 108.9, O_{27}–S_{25}–N_{28} = 104.9, $O_{27,26}$–S_{25}–C_{22} = 107.9–108.3, N_{28}–S_{25}–C_{22} = 107.9, C_{30}–N_{28}–S_{25} = 123.0° reported by Lasibal et al. [40] are in agreement with our values.

At C_3 position, the bond angles C_4–C_3–C_2, C_4–C_3–C_{12}, and C_2–C_3–C_{12} are 119.2, 119.3, and 121.5° respectively. This asymmetry in angles reveals the interaction between azomethane and the phenyl groups. At C_{15} position the angles C_{17}–C_{15}–N_{14} is increased by 3° and C_{16}–C_{15}–N_{14} is reduced by 2.2° from 120° which reveals the interaction between N_{14} and H_{21} atoms. At C_{22} position C_{20}–C_{22}–S_{25} = 120.1° and C_{20}–C_{22}–C_{18} = 121.2° which shows the interaction between SO_2 group with H_{24} atom. At N_{28} position, S_{25}–N_{28}–H_{29} is reduced by 7.8° and S_{25}–N_{28}–C_{30} is increased by 6.8° from 120° which shows the interaction between H_{29} and O_{27}. The C_{12} = N_{14} moiety is slightly tilted from monosubstituted phenyl ring as is evident from the torsion angles C_5–C_4–C_3–C_{12} = −179.8, C_4–C_3–C_{12}–N_{14} = −179.0, C_1–C_2–C_3–C_{12} = 179.9, C_2–C_3–C_{12}–N_{14} = 177.4° and is more tilted from the para substituted phenyl ring as is evident from the torsion angles C_{20}–C_{17}–C_{15}–N_{14} = 178.6, C_{17}–C_{15}–C_{14}–C_{12} = 42.1, C_{18}–C_{16}–C_{15}–N_{14} = 179.6, and C_{16}–C_{15}–N_{14}–C_{12} = −140.4°. The torsion angle S_{25}–N_{28}–C_{30}–N_{32} = −169.9 and S_{25}–N_{28}–C_{30}–N_{31} = 12.6°, which shows that the N_{31} and N_{32} atoms are in different planes.

Nonlinear optics deal with the interaction of applied electromagnetic fields in various materials to generate new electromagnetic fields, altered in wavenumber, phase, or other physical properties [41]. Organic molecules able to manipulate photonic signals efficiently are of importance in technologies such as optical communication, optical computing, and dynamic image processing [42, 43]. In this context, the dynamic first hyperpolarizability of the title compound is also calculated in the present study. The first hyperpolarizability (β_0) of this novel molecular system is calculated using B3LYP method, based on the finite field approach. In the presence of an applied electric field, the energy of a system is a function of the electric field. First hyperpolarizability is a third rank tensor that can be described by a 3 × 3 × 3 matrix. The 27 components of the 3D matrix can be reduced to 10 components due to the Kleinman symmetry [44]. The components of β are defined as the coefficients in the Taylor series expansion of the energy in the external electric field. When the electric field is weak and homogeneous, this expansion becomes

$$E = E_0 - \sum_i \mu_i F_i - \frac{1}{2}\sum_{ij} \alpha_{ij} F^i F^j - \frac{1}{6}\sum_{ijk} \beta_{ijk} F^i F^j F^k - \frac{1}{24}\sum_{ijkl} \gamma_{ijkl} F^i F^j F^k F^l + \cdots, \quad (1)$$

where E_0 is the energy of the unperturbed molecule, F^i is the field at the origin, μ_i, α_{ij}, β_{ijk}, and γ_{ijkl} are the components of dipole moment, polarizability, the first hyperpolarizabilities, and second hyperpolarizabilities, respectively. The calculated first hyperpolarizability of the title compound is 6.25 × 10^{-30} esu, which is comparable with the reported values of similar derivatives, but experimental evaluation of this data is not readily available. Kucharski et al. [45] reported the first hyperpolarizability of certain sulfonamide amphiphiles by calculation and hyper-Rayleigh scattering in the range 0.2156–0.189 × 10^{-30} esu. We conclude that the title compound is an attractive object for future studies of nonlinear optical properties.

5. Conclusion

The FT-IR and FT-Raman spectrum of the title compound were recorded and analyzed. The molecular geometry and vibrational wavenumbers were calculated using HF and DFT methods, and the optimized geometrical parameters (B3LYP) are in agreement with that of reported similar derivatives. The red shift of the N–H stretching band in the infrared spectrum from the computed wavenumber indicates the weakening of the N–H bond. The calculated first hyperpolarizability is comparable with the reported value of similar derivative and may be an attractive object for further studies of non linear optics. Potential energy surface scan studies have been carried out to understand the stability of planar and non planar structures of the molecule.

References

[1] A. K. Biswas, G. S. Rao, N. Kondaiah, A. S. R. Anjaneyulu, and J. K. Malik, "Simple multiresidue method for monitoring of trimethoprim and sulfonamide residues in Buffalo meat by high-performance liquid chromatography," *Journal of Agricultural and Food Chemistry*, vol. 55, no. 22, pp. 8845–8850, 2007.

[2] C. T. Supuran, "Carbonic anhydrases: novel therapeutic applications for inhibitors and activators," *Nature Reviews Drug Discovery*, vol. 7, no. 2, pp. 168–181, 2008.

[3] C. T. Supuran, "Diuretics: from classical carbonic anhydrase inhibitors to novel applications of the sulfonamides," *Current Pharmaceutical Design*, vol. 14, no. 7, pp. 641–648, 2008.

[4] C. Temperini, A. Cecchi, A. Scozzafava, and C. T. Supuran, "Carbonic anhydrase inhibitors. Comparison of chlorthalidone, indapamide, trichloromethiazide, and furosemide X-ray crystal structures in adducts with isozyme II, when several water molecules make the difference," *Bioorganic and Medicinal Chemistry*, vol. 17, no. 3, pp. 1214–1221, 2009.

[5] J. Y. Winum, C. Temperini, K. El Cheikh et al., "Carbonic anhydrase inhibitors: clash with Ala65 as a means for designing inhibitors with low affinity for the ubiquitous isozyme II,

exemplified by the crystal structure of the topiramate sulfamide analogue," *Journal of Medicinal Chemistry*, vol. 49, no. 24, pp. 7024–7031, 2006.

[6] Z. Guo and P. J. Sadler, "Metals in medicine," *Angewandte Chemie*, vol. 38, no. 11, pp. 1513–1531, 1999.

[7] R. X. Yuan, R. G. Xiong, and Z. F. Chen, "Crystal structure of zinc(II) 2-sulfanilamidopyrimidine: a widely used topical burn drug," *Journal of the Chemical Society-Dalton Transactions*, vol. 6, no. 774, p. 776, 2001.

[8] T. H. Maren, "Relatons between structure and biological activity of sulfonamides," *Annual Review of Pharmacology and Toxicology*, vol. 16, pp. 309–327, 1976.

[9] C. T. Supuran, A. Scozzafava, and A. Mastrolorenzo, "Bacterial proteases: current therapeutic use and future prospects for the development of new antibiotics," *Expert Opinion on Therapeutic Patents*, vol. 11, no. 2, pp. 221–259, 2001.

[10] A. E. Boyd, "Sulfonylurea receptors, ion channels, and fruit flies," *Diabetes*, vol. 37, no. 7, pp. 847–850, 1988.

[11] T. Owa and T. Nagasu, "Novel sulphonamide derivatives for the treatment of cancer," *Expert Opinion on Therapeutic Patents*, vol. 10, no. 11, pp. 1725–1740, 2000.

[12] C. W. Thornber, "Isosterism and molecular modification in drug design," *Chemical Society Reviews*, vol. 8, no. 4, pp. 563–580, 1979.

[13] U. K. Singh, S. N. Pandeya, A. Singh, B. K. Srivastava, and M. Pandey, "Synthesis and antimicrobial activity of Schiff's and N-mannich bases of isatin and its derivatives with 4-amino-N-carbamimidoyl benzene sulfonamide," *International Journal of Pharmaceutical Sciences and Drug Research*, vol. 2, no. 2, pp. 151–154, 2010.

[14] X. Liu, L. Liu, X. Lu, J. Zheng, W. Wang, and Y. Fang, "Interference second harmonic generation investigation of the chromophore orientation of hemicyanine dye molecules in a Langmuir-Blodgett monolayer," *Thin Solid Films*, vol. 217, no. 1-2, pp. 174–177, 1992.

[15] Y. Miyamoto, K. Kaifu, T. Koyano, M. Saito, and M. Kato, "Second harmonic generation from mixed Langmuir-Blodgett films of N-acyl-p-nitroaniline and its homologous amphiphile," *Thin Solid Films*, vol. 210-211, pp. 178–181, 1992.

[16] M. J. Frisch, G. W. Trucks, H. B. Schlegel et al., *Gaussian 03, Revision C.02*, Gaussian, Inc, Wallingford, Conn, USA, 2004.

[17] J. B. Foresman, *Expploring Chemistry with Electronic Structure Methods: A Guide to Using Gaussian*, Gaussian Inc., Pittsburgh, Pa, USA, 1996.

[18] J. M. L. Martin and C. Van Alsenoy, *GAR2PED, A Program to obtain a Potential Energy Distribution from a Gaussian Archive Record*, University of Antwerp, Brussels, Belgium, 2007.

[19] P. Flukiger, H. P. Luthi, S. Portmann, and J. Weber, *MOLEKEL 4.3, Swiss Centre for Scientific Computing*, Manno, Lugano, Switzerland, 2002.

[20] S. Portmann and H. P. Lüthi, "MOLEKEL: an interactive molecular graphics tool," *Chimia*, vol. 54, no. 12, pp. 766–769, 2000.

[21] N. P. G. Roges, *A Guide to the Complete Interpretation of the Infrared Spectra of Organic Structures*, John Wiley & Sons, New York, NY, USA, 1994.

[22] Z. H. Chohan, M. H. Youssoufi, A. Jarrahpour, and T. B. Hadda, "Identification of antibacterial and antifungal pharmacophore sites for potent bacteria and fungi inhibition: indolenyl sulfonamide derivatives," *European Journal of Medicinal Chemistry*, vol. 45, no. 3, pp. 1189–1199, 2010.

[23] A. Hangen, A. Bodoki, L. Orpean, G. Alzuet, M. Liu-Gonzalez, and J. Borras, "Synthesis, crystallographic and spectroscopic characterization and magnetic properties of dimer and monomer ternary copper(II) complexes with sulfonamide derivatives and 1,10-phenanthroline. Nuclease activity by the oxidative mechanism," *Polyhedron*, vol. 29, no. 4, pp. 1305–1313, 2010.

[24] I. Yalcin, E. Sener, T. Ozden, S. Ozden, and A. Akin, "Synthesis and microbiological activity of 5-methyl-2-[*p*-substituted phenyl]benzoxazoles," *European Journal of Medicinal Chemistry*, vol. 25, no. 8, pp. 705–708, 1990.

[25] N. B. Colthup, L. H. Daly, and S. E. Wiberly, *Introduction to Infrared and Raman Spectroscopy*, Academic Press, New York, NY, USA, 1975.

[26] C. Y. Panicker, H. T. Varghese, K. C. Mariamma et al., "Spectroscopic investigations and computational study of 2-[acetyl(4-bromophenyl)carbamoyl]-4-chlorophenyl acetate," *Journal of Raman Spectroscopy*, vol. 41, no. 6, pp. 707–716, 2010.

[27] L. J. Bellamy, *The IR Spectra of Complex Molecules*, John Wiley & Sons, New York, NY, USA, 1975.

[28] A. Spire, M. Barthes, H. Kellouai, and G. De Nunzio, "Far-infrared spectra of acetanilide revisited," *Physica D*, vol. 137, no. 3-4, pp. 392–401, 2000.

[29] M. Barthes, G. DeNunzio, and G. Ribet, "Polarons or proton transfer in chains of peptide groups?" *Synthetic Metals*, vol. 76, no. 1–3, pp. 337–340, 1996.

[30] C. Y. Panicker, K. R. Ambujakshan, H. T. Varghese et al., "FT-IR, FT-Raman and DFT calculations of 3-[(4-fluorophenyl)methylene]amino-2-phenylquinazolin-4(3H)-one," *Journal of Raman Spectroscopy*, vol. 40, no. 5, pp. 527–536, 2009.

[31] P. L. Anto, C. Y. Panicker, H. T. Varghese et al., "Vibrational spectroscopic studies and ab initio calculations of 5-methyl-2-(P-fluorophenyl)benzoxazole," *Spectrochimica Acta A*, vol. 67, pp. 744–749, 2007.

[32] K. R. Ambujakshan, V. S. Madhavan, H. T. Varghese et al., "Vibrational spectroscopic studies and ab initio calcula-tions of 5-methyl-2-(*p*-methylaminophenyl)benzoxazole," *Spectrochimica Acta A*, vol. 69, no. 3, pp. 782–788, 2008.

[33] P. Sett, N. Paul, S. Chattopadhyay, and P. K. Mallick, "Molecular structures in the excited states of 2- and 4-benzylpyridine," *Journal of Raman Spectroscopy*, vol. 30, no. 4, pp. 277–287, 1999.

[34] J. H. S. Green, "Vibrational spectra of benzene derivatives-IV. Methylphenyl sulphide, diphenyl sulphide, diphenyl disulphide and diphenyl sulphoxide," *Spectrochimica Acta A*, vol. 24, no. 10, pp. 1627–1637, 1968.

[35] J. Coates, "Interpretation of infrared spectra, a practical approach," in *Encyclopedia of Analytical Chemistry*, R. A. Meyers, Ed., John Wiley & Sons, Chichester, UK, 2000.

[36] G. Varsanyi, *Assignments of Vibrational Spectra of Seven Hundred Benzene Derivatives*, John Wiley & Sons, New York, NY, USA, 1974.

[37] D. Philip, A. John, C. Y. Panicker, and H. T. Varghese, "FT-Raman, FT-IR and surface enhanced Raman scattering spectra of sodium salicylate," *Spectrochimica Acta A*, vol. 57, no. 8, pp. 1561–1566, 2001.

[38] B. T. Loughrey, M. L. Williams, and P. C. Healy, "4-(Benzylideneamino)benzenesulfonamide," *Acta Crystallographica E*, vol. 65, pp. 2087–2096, 2009.

[39] V. Petrov, V. Petrova, G. V. Girichev, H. Oberhammer, N. I. Giricheva, and S. Ivanov, "Molecular structure and conformations of benzenesulfonamide: gas electron diffraction and

quantum chemical calculations," *Journal of Organic Chemistry*, vol. 71, no. 8, pp. 2952–2956, 2006.

[40] E. Labisbal, L. Rodriguez, A. Sousa-Pedrares et al., "Synthesis, characterisation and X-ray structures of diorganotin(IV) and iron(III) complexes of dianionic terdentate Schiff base ligands," *Journal of Organometallic Chemistry*, vol. 691, no. 7, pp. 1321–1332, 2006.

[41] Y. R. Shen, *The Principles of Nonlinear Optics*, John Wiley & Sons, New York, NY, USA, 1984.

[42] P. V. Kolinsky, "New materials and their characterization for photonic device applications," *Optical Engineering*, vol. 31, pp. 1676–1684, 1992.

[43] D. F. Eaton, "Nonlinear optical materials," *Science*, vol. 253, no. 5017, pp. 281–287, 1991.

[44] D. A. Kleinman, "Nonlinear dielectric polarization in optical media," *Physical Review*, vol. 126, no. 6, pp. 1977–1979, 1962.

[45] S. Kucharski, R. Janik, and P. Kaatz, "First hyperpolarizability of new sulfonamide amphiphiles by calculation, and hyper-Rayleigh scattering," *Journal of Materials Chemistry*, vol. 9, no. 2, pp. 395–401, 1999.

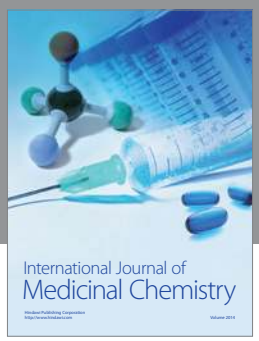

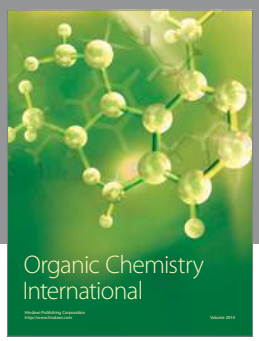

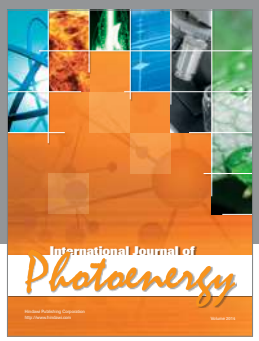

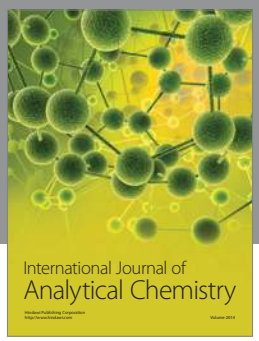

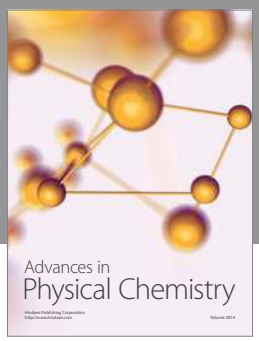

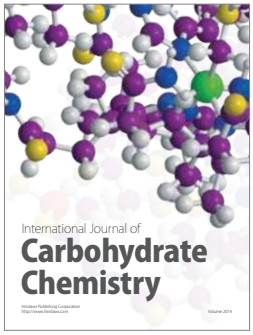

Hindawi
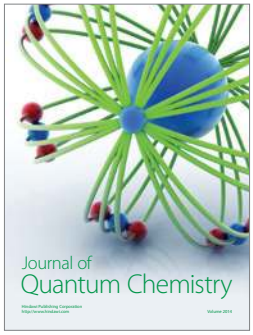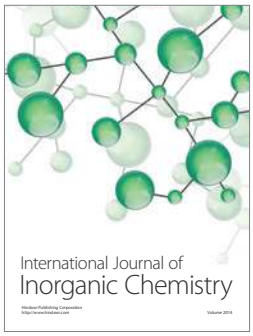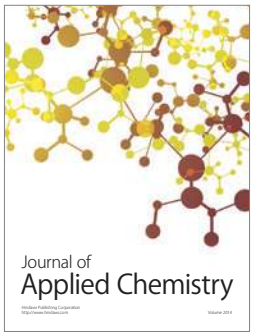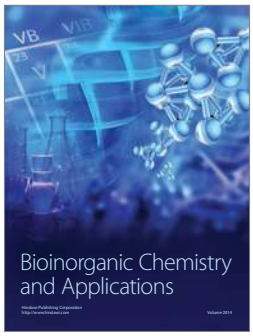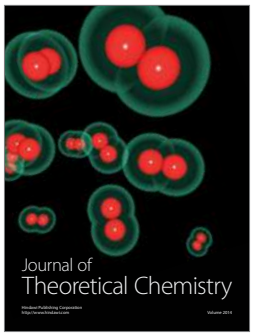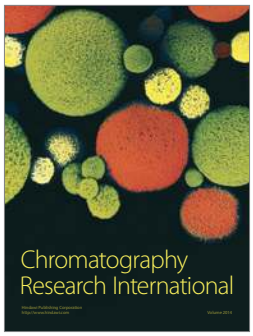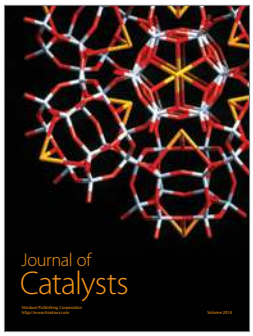
Submit your manuscripts at
http://www.hindawi.com